

CONSIDERATIONS ON THE ACQUISITION, PROCESSING, AND MATHEMATICAL INTERPRETATION OF THE GEOREFERENCING PROCESS

*Assoc.prof. PhD TUDOR BORȘAN, prof.PhD LEVENTEDIMEN,
assoc.prof. PhD ANDREEA RAMONA BEGOV, lecturer PhD SILVIA ALEXANDRA DREGHICI
"1 Decembrie 1918" University of Alba Iulia, Romania*

ABSTRACT: *The study addresses the georeferencing process from an integrated perspective, examining the stages of acquisition, processing, and mathematical interpretation of spatial data. The control points used, defined virtually within the digital environment, function as coordinate-bearing elements that underpin the alignment of the raster image within a coherent projection system. The georeferencing procedure is analyzed both procedurally and mathematically, through the determination of transformation parameters and the evaluation of residual errors using the RMS indicator. The results emphasize the importance of correct data preprocessing and the relevance of mathematical interpretation in ensuring the geospatial accuracy of georeferenced imagery.*

Keywords: *georeferencing; ground control points; transformation; translation; rotation; scale; rectify; RMS; standard deviation;*

Introduction

In the current context of geospatial technology development, the georeferencing process represents one of the essential stages in the processing and integration of raster imagery within GIS environments. Through georeferencing, an image initially lacking spatial reference acquires a real position within a coordinate system, enabling overlay, analysis, and correlation with other geospatial datasets. Although, at first glance, this process may appear to be a simple geometric adjustment, in essence it involves a complex set of mathematical transformations, methodological decisions, and precision assessments.

The present study aims to illustrate the logical stages of the georeferencing workflow, starting with the acquisition of virtual control points, followed by the processing of their coordinates and conversion from DMS (degrees, minutes, seconds) into DD (decimal degrees), and continuing with the transformation of the reference system from WGS 84 to the local datum — Dealul Piscului 1970 — and the computation of planar coordinates in the national Stereo 70 projection. The main objective of this approach is to highlight the relationship between the practical and theoretical components of georeferencing — from the selection of control points and the choice

of a first-order affine transformation model, to the mathematical interpretation of transformation parameters (a, b, c, d, e, f) and the evaluation of the RMS error. Furthermore, the study proposes an accessible methodological approach based on the integration of all steps into a unified processing workflow, facilitating the understanding of the georeferencing process both technically and conceptually.

Workflow from data acquisition to the mathematical interpretation of spatial transformations

In this context, the main stages of the georeferencing process are presented, beginning with the identification of the area of interest and the extraction of virtual control points, followed by the conversion of their coordinates from DMS (degrees, minutes, seconds) into DD (decimal degrees), and continuing with the conversion and transformation of coordinates between reference systems (WGS 84 – Dealul Piscului 1970). The workflow proceeds to the calculation of rectangular coordinates in the Stereo 70 national projection system and the mathematical analysis of the transformation parameters. Overall, the sequence illustrates the transition of geospatial information from acquisition to integration and geometric validation (Fig. 1).

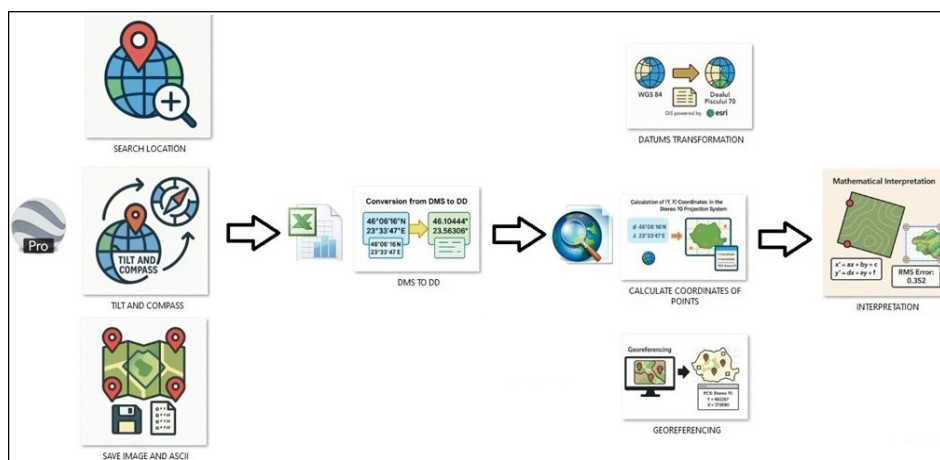


Fig. 1. Georeferencing process information flow

Data acquisition

The acquisition stage represents the initial and defining moment of the georeferencing process, in which the geometric foundation of the entire processing workflow is established. Within this phase, data are obtained through the three-dimensional visualization environment provided by the Google Earth platform, which allows a progressive and controlled zooming approach toward the Area of Interest (AOI). This approach is facilitated by deploying a predefined spatial template, intended to fix the analytical framework and delimit the working space according to the thematic objective of the study. It is also noteworthy that the observer–image

relationship is characterized by a dual perspective; therefore, a visualization command is initiated so that both orthographic and azimuthal perspectives are captured simultaneously.

The Google Earth platform provides a dynamic observation environment, where the digital elevation model (DEM) and high-resolution satellite imagery can be visually correlated, allowing the user to establish location markers (placemarks) through an assisted selection process.

These markers function as virtual control points, carrying geographic coordinate information that will serve as the primary references in the subsequent georeferencing process (Fig. 2, 3).



Fig. 2. Use of the spatial template and validation of observation perspectives

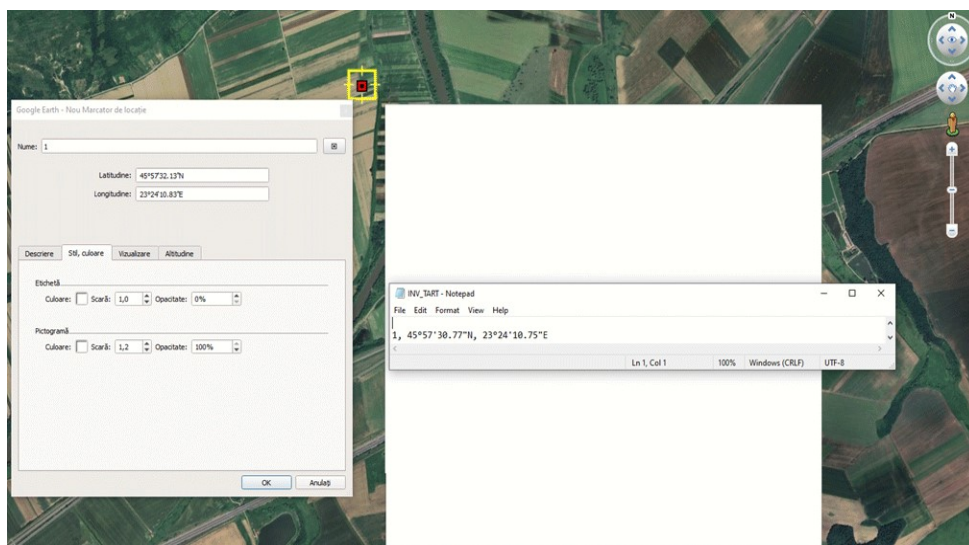


Fig. 3. Placement of placemarks and extraction of coordinate sets in DMS format

After identifying and placing the selected points, the geographic coordinate values are recorded for each marker. The coordinates are extracted in degrees–minutes–seconds (DMS) format, corresponding to the WGS 84 reference system, and organized into an ASCII-type file to ensure interoperability with other applications. This file contains, for each control point, a triplet of information—ID, latitude, and longitude—which subsequently allows automatic conversion into other numerical formats. The final stage of the acquisition phase consists of the simultaneous saving of the two fundamental entities: the raster image (as observed within the platform) and the ASCII file containing the DMS coordinate values. These resources are intended for further processing in Microsoft Excel, where the numerical conversion of coordinates into decimal degrees (DD) will be performed, a crucial step in ensuring compatibility with the GIS environment.

Numerical preprocessing of coordinate data

After exporting the data in ASCII format, the next stage consists of processing the geographic coordinates in a tabular environment, Microsoft Excel being the most frequently used due to its flexibility in handling formulas and numerical conversions. The objective of this phase is to convert the coordinate values from DMS (degrees, minutes, seconds) into DD (decimal degrees), the format compatible with most GIS applications.

The ASCII file exported from Google Earth is opened or imported into Microsoft Excel using the Open → All Files function, which ensures recognition of all file types, followed by the selection of the appropriate delimiter (a comma, in this case) (Fig. 4).

1	45°57'30.77"N	23°24'10.75"E
2	45°57'31.47"N	23°26'13.77"E
3	45°56'11.72"N	23°26'16.29"E
4	45°56'12.55"N	23°24'10.94"E

Fig. 4. Delimitation of tabular cells for numerical conversion

To facilitate the calculation required for obtaining the DD format, the DMS values must be separated into their numerical components (degrees, minutes and seconds), while removing the special characters (° "). (Fig. 5)

After extracting the numerical components, the conversion is performed using the standard formula: (Fig. 6)

After the conversion, the data can be exported in CSV or XLS format for subsequent interpretation within the GIS environment. This stage ensures data cleaning and the numerical standardization required to prevent errors during GIS processing.

Raster georeferencing

After obtaining the geographic coordinates expressed in decimal degrees (DD), defined within the global reference system WGS 84, an additional transformation was required to align

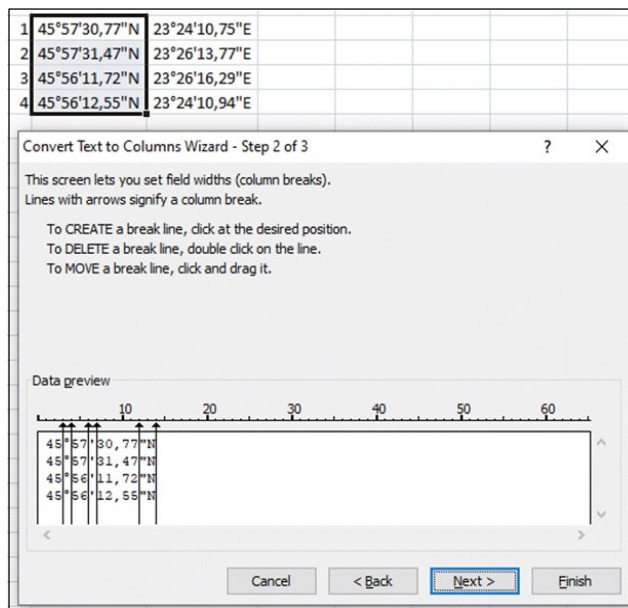


Fig. 5. Cell splitting

$$DD = G + \frac{M}{60} + \frac{S}{3600}$$

1	45°57'30,77"N	23°24'10,75"E	45	57	30,77	=D2+E2/60+F2/3600
2	45°57'31,47"N	23°26'13,77"E	45	57	31,47	
3	45°56'11,72"N	23°26'16,29"E	45	56	11,72	
4	45°56'12,55"N	23°24'10,94"E	45	56	12,55	

						LAT_DD
1	45°57'30,77"N	23°24'10,75"E	45	57	30,77	45,95855
2	45°57'31,47"N	23°26'13,77"E	45	57	31,47	45,95874
3	45°56'11,72"N	23°26'16,29"E	45	56	11,72	45,93659
4	45°56'12,55"N	23°24'10,94"E	45	56	12,55	45,93682

Fig. 6. Carrying out the conversion

them with the national geodetic system of Romania — Dealul Piscului 1970. This datum transformation ensures spatial compatibility between globally referenced coordinates and the local projection system used in Romanian cartography and topography (Fig. 7).

The Helmert model establishes the spatial relationship between the two reference systems according to the following equations:

$$\begin{aligned} X_2 &= T_x + (1 + m)(X_1 + r_z Y_1 - r_y Z_1) \\ Y_2 &= T_y + (1 + m)(-r_z X_1 + Y_1 + r_x Z_1) \\ Z_2 &= T_z + (1 + m)(r_y X_1 - r_x Y_1 + Z_1) \end{aligned}$$

This transformation correlates the global WGS 84 ellipsoid with the Krasovsky ellipsoid used within the Dealul Piscului 1970 datum. In order to validate the results obtained in the GIS environment, an analytical calculation of the

rectangular coordinate sets was performed based on the applied transformation (Fig. 8).

After determining the rectangular coordinates in the Stereo 70 system, the raster image obtained from Google Earth was imported into the GIS environment, where the actual georeferencing procedure was carried out. The process consisted in establishing a spatial correspondence between the points identified on the image and their real coordinates within the projection system. For this stage, a first-order affine (polynomial) transformation was used, which enables a flexible geometric adjustment while preserving properties such as parallelism and collinearity. The mathematical model of the affine transformation is expressed by the system of equations:

$$\begin{aligned} x' &= ax + by + c \\ y' &= dx + ey + f \end{aligned}$$

a, e – scaling parameters
b, d – rotation parameters
c, f – translation parameters

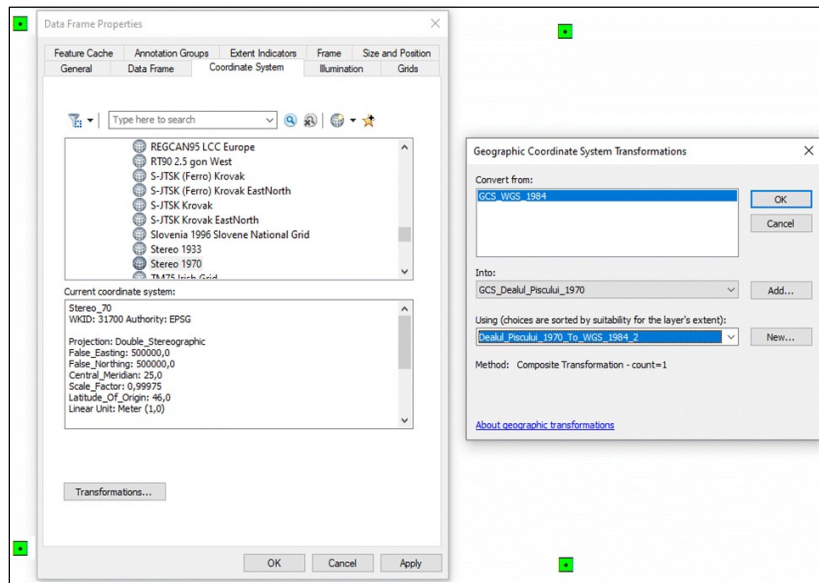


Fig. 7. Performing the datum transformation

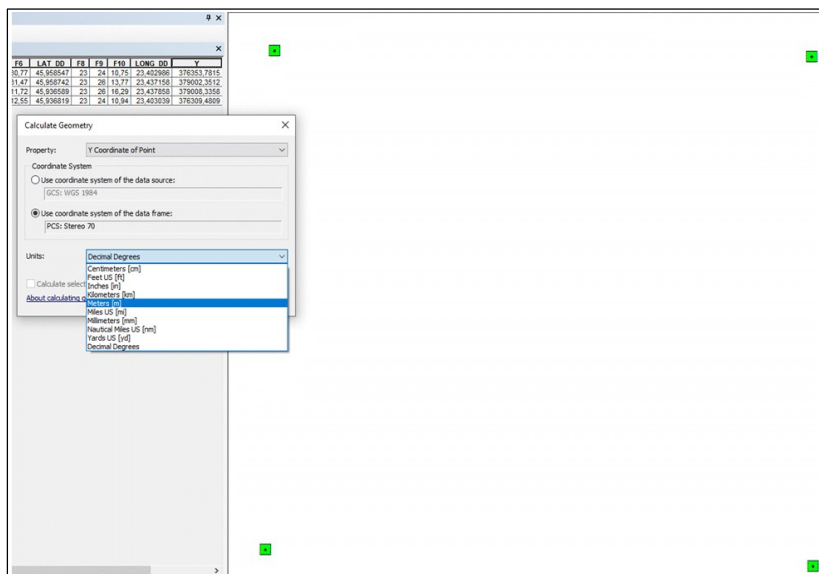


Fig. 8. Calculation of projected coordinates for the control points

The solution of the equation system was performed based on the four previously defined control points (GCPs), by minimizing the residual errors associated with each point. Subsequently, the RMS (Root Mean Square) error was calculated, an indicator expressing the average deviation between the theoretical point positions and those resulting after transformation.

The resulting RMS value reflects the overall geometric accuracy of the georeferencing process and the degree of conformity between the raster

image and the coordinate system used as reference (Fig. 9, 10).

Results and discussions

The georeferencing of the raster image was carried out by means of a first-order (affine) transformation, using four Ground Control Points (GCPs) strategically distributed both along the perimeter and within the interior of the area of interest, in order to ensure optimal geometric stability of the model.

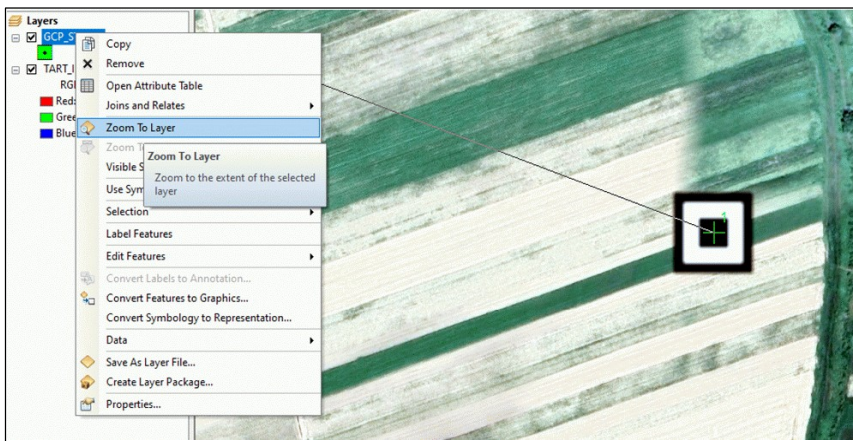


Fig. 9. Handling of Ground Control Points

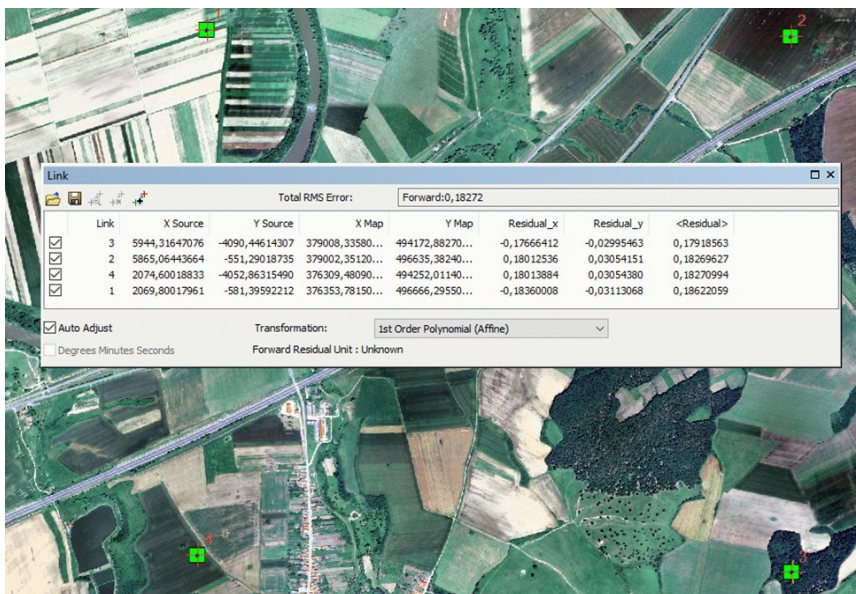


Fig. 10. Evaluation of the RMS error

The parameters calculated for each control point indicate residual values ranging between 0.17 and 0.18 units, resulting in a total Root Mean Square error of RMS Total = 0.18272.

This value falls below the 0.2 threshold which, according to the specialized literature (Burrough & McDonnell, 1998; Maling, 1992), defines a high-quality georeferencing result for cartographic products derived from medium-resolution satellite imagery. The residuals represent the differences between the modeled position and the actual position of each control point, forming the basis for RMS computation:

$$RMS = \sqrt{\frac{\sum_{i=1}^n (Residual_{x_i}^2 + Residual_{y_i}^2)}{n}}$$

The distribution of residual values suggests a slight local anisotropy caused by inherent raster deformation near the peripheral regions, where greater inter-point distances tend to amplify projection-related distortions. The larger residuals observed for control points 3 and 4 may be attributed to their proximity to the image boundaries, where deformation effects resulting from the WGS 84–Stereo 70 conversion become more pronounced. From a mathematical standpoint, model stability is confirmed by the consistency of the individual RMS values, which fall within a maximum variation of ± 0.005 units from the overall mean. Consequently, systematic errors are negligible, and the model can be considered both convergent and robust, suitable for GIS

applications at medium topographic scales (1:5,000 – 1:25,000). The statistical analysis of the residuals obtained during the georeferencing process highlights a coherent distribution of deviations relative to the theoretical control point positions. The arithmetic mean of residuals along the X and Y directions reflects a generally well-aligned transformation, without significant systematic displacement (1).

To evaluate the dispersion of the georeferencing errors, the standard deviations of the residuals along the x- and y-directions were calculated, according to the following relations (2):

$$\begin{aligned} X &= \{0.1766412, 0.1801236, 0.1830844, 0.1827390\} & \bar{X} &= \frac{\sum X_i}{4} = 0.18064705 \\ Y &= \{0.02995463, 0.03455114, 0.03034108, 0.02225324\} & \bar{Y} &= \frac{\sum Y_i}{4} = 0.02927502 \end{aligned} \quad (1)$$

$$\begin{aligned} \sigma_X &= \sqrt{\frac{\sum (X_i - \bar{X})^2}{3}} = \sqrt{\frac{(-0.00400585)^2 + (-0.00052345)^2 + (0.00243735)^2 + (0.00209195)^2}{3}} = \mathbf{0.00298}. \\ \sigma_Y &= \sqrt{\frac{\sum (Y_i - \bar{Y})^2}{3}} = \sqrt{\frac{(0.00067961)^2 + (0.00527612)^2 + (0.00106606)^2 + (-0.00702178)^2}{3}} = \mathbf{0.00512}. \end{aligned} \quad (2)$$

The standard deviation values indicate a low dispersion of the errors, confirming a high internal stability of the affine transformation model. However, a slight increase in variability is observed along the west–east direction, suggesting a possible influence of the source raster resolution or the positioning of control points in areas with fragmented relief or abrupt transitions between surfaces exhibiting different reflectance.

$$\begin{aligned} CV_X &= \frac{\sigma_X}{\bar{X}} \cdot 100\% \approx \mathbf{1.65\%}, \\ CV_Y &= \frac{\sigma_Y}{\bar{Y}} \cdot 100\% \approx \mathbf{17.5\%}. \end{aligned}$$

The ratio between the standard deviation and the mean residuals (1.65% for x and 17.5% for y) confirms the predominance of geometric stability along the east–west axis, with a more pronounced variability in the vertical or meridional direction. From a methodological standpoint, the low standard deviation values and a global RMS of 0.1827 support the conclusion that the georeferencing meets the geometric accuracy

criteria associated with a first-order model, without requiring a higher-order transformation. The relatively uniform distribution of errors and the absence of marked directional trends confirm an adequate fit between the reference coordinate set and the transformed coordinates.

Conclusions

The results confirm that the georeferencing process, performed using a set of four virtual control points, ensures a coherent geometric alignment between the source image and the reference coordinate system. The low residual and

standard deviation values indicate a high internal stability of the affine model, with minimal spatial variation of distortions. The observed differences suggest the presence of secondary factors — such as local topographic effects, variations in raster resolution, or an uneven distribution of control points - which may locally influence transformation quality. Even so, the global RMS value of 0.1827 falls within the acceptable limits for medium-precision cartographic products, confirming that the first-order (affine) transformation was sufficient for positional correction of the image. From a methodological perspective, the results demonstrate the effectiveness of integrating coordinate conversion (DMS–DD), datum transformation (WGS 84 – Dealul Piscului 70), and mathematical error evaluation within a unified georeferencing workflow. This approach underscores the importance of numerical post-processing analysis (residuals, deviations, RMS) for the rigorous validation of derived spatial products and for ensuring the metric traceability of geospatial data.

References

1. Borșan, T., *Topografie arheologică i GIS*, Editura Risoprint, Cluj-Napoca, 2015;
2. T. Borșan, I. Ienciu, L. Dimen, L. Oprea, G. E. Voicu: *An Exploratory Analysis Of Topographic And Archeological Data Gathered During Systematic Research*, 13th SGEM GeoConference on Informatics, Geoinformatics And Remote Sensing, www.sgem.org, SGEM2013 Conference Proceedings, ISBN 978-954-91818-9-0 / ISSN 1314-2704, June 16-22, 2013, Vol. 1, 629 - 636;
3. Tudor Borșan, Ioan Ienciu, Luciana Oprea, Larisa Ofelia Filip, *Metodologia de punere în practică a georeferențierii utilizând transformarea afină*, Revista Pangeea, Vol. 15, 9-13, 2015;
4. Andreas Hackeloeer, Klaas Klasing, Jukka M. Krisp & Liqiu Meng (2014) *Georeferencing: a review of methods and applications*, Annals of GIS, 20:1, 61-69, DOI: 10.1080/19475683.2013.868826;
5. Herbei, M.V.; Ciolac, V.; Smuleac, A.; Nistor, E.; Ciolac, L. *Georeferencing of topographical maps using the software ARCGIS*. Res. J. Agric. Sci. 2010, 42, 595–606;
6. Hill, L. L. 2006. *Georeferencing: The Geographic Associations of Information*, 2. Cambridge, MA: MIT Press;
7. Legat, K. *Approximate direct georeferencing in national coordinates*. ISPRS Journal of Photogrammetry & Remote Sensing 60, 239–255, 2006;
8. M. Simon, C.A. Popescu, Loredana Copăcean, Luminița Cojocariu, *Cad and GIS techniques in georeferencing maps for the identification and mapping of meadows in Arad County*, Research Journal of Agricultural Science, 49 (4), 2017, 276-283;
9. Sisman, A., *An experimental design approach on georeferencing*, BCG - Boletim de Ciências Geodésicas - On-Line version, ISSN 1982-2170 <http://dx.doi.org/10.1590/S1982-21702014000300031>, 548-561;
10. Zheng, Y., Z. Zha, and T. Chua. 2011. *Research and Applications on Georeferenced Multimedia: A Survey*. Multimedia Tools and Applications 51 (1): 77–98.